On the Relationship between Stress and Elastic Strain for Porous and Fractured Rock

Hui-Hai Liu*, Jonny Rutqvist and James G. Berryman

Earth Sciences Division
Lawrence Berkeley National Laboratory
Berkeley, CA 94720

Submitted to
International Journal of Rock Mechanicals & Mining Science & Mining Sciences

---

*Corresponding author. Tel: +1-510-486-6452; fax: +1-510-486-5686. E-mail address: hhliu@lbl.gov

Abstract

Modeling the mechanical deformations of porous and fractured rocks requires a stress-strain relationship. Experience with inherently heterogeneous earth materials suggests that different varieties of Hook's law should be applied within regions of the rock having significantly different stress-strain behavior, *e.g.*, such as solid phase and various void geometries. We apply this idea by dividing a rock body conceptually into two distinct parts. The natural strain (volume change divided by rock volume at the current stress state), rather than the engineering strain (volume change divided by the unstressed rock volume), should be used in Hooke's law for accurate modeling of the elastic deformation of that part of the pore volume subject to a relatively large degree of relative deformation (*i.e.*, cracks or fractures). This approach permits the derivation of constitutive relations between stress and a variety of mechanical and/or hydraulic rock properties. We show that the theoretical predictions of this method are generally consistent with empirical expressions (from field data) and also laboratory rock experimental data.

Keywords: Stress-strain relationship; Hooke's law; Constitutive relationships

1. Introduction

Mechanical deformation processes in porous and fractured rock and their coupling with thermal and hydrological processes are important for many applications [1], including geothermal energy development [2,3], oil and gas extraction [4], nuclear waste disposal [5,6], geological sequestration of carbon dioxide [7], and deep well injection of liquid and solid wastes [8,9]. With the significant advancement of computer technology in recent decades, numerical models have been increasingly employed for evaluating coupled mechanical, hydrological, and thermal processes associated with these applications [10].

The stress-strain relationship is fundamental for modeling mechanical deformation and the associated coupled processes in porous and fractured rock. Hooke's law has been generally used to describe this stress-strain relationship for elastic mechanical processes. Hooke's law, an approximation, states that the amount by which a material (e.g., rock) body is deformed (the strain) is linearly related to the force (stress) causing the deformation. However, the current application of the Hooke's law to porous and fractured rock is not without questions. Strictly speaking, the proportionality in the observed stress-strain relationship should be constant if the current application of Hooke's law is perfectly valid. However, some studies indicate that the proportionality is not always constant, but rather stress-dependent in many cases [11,12]. A number of efforts have been made to relate this stress-dependent behavior to the microstructures of "cracks" in porous rock [13,14,15]. An excellent review of these efforts is provided in a chapter entitled *Micromechanical Models* in Jaeger et al. [16]. Because it is generally difficult to characterize small-scale structures accurately and then relate their properties to large-

scale mechanical properties that are of practical interest, it is desirable to have a macroscopic-scale theory that does not rely on the detailed description of small-scale structures, and that can physically incorporate the stress-dependent behavior of relevant mechanical properties. The first objective of this study is to develop a theory of this kind within the framework of Hooke's law.

For a stress-sensitive rock, the stress-strain relationship largely determines the relationships between stress and other rock mechanical/hydraulic properties, and these relationships control the degree of coupling between mechanical and hydrological processes [7,17]. However, the commonly used relationships between stress and hydraulic properties (such as porosity and fracture aperture) are generally empirical [7,18]. The second objective of this study is to derive mathematical formulations for these constitutive relationships based on our newly proposed stress-strain relationship.

This paper is organized as follows. We first present the development of a stress-strain relationship, and then derive constitutive relationships between stress and hydraulic/mechanic properties. Comparisons are then made between these relationships and the corresponding empirical expressions and experimental data, to evaluate the validity of our theoretical approach.

2. Theory

This section presents a new stress-strain relationship for porous and fractured rock based on Hooke's law. For simplicity, we mainly consider the relationship here for the volumetric strain, although our results can be easily extended to other types of strains.

Assume that a uniformly distributed force is imposed on the surface of a homogeneous and isotropic material body subject to elastic deformation. In this case, Hooke's law can be expressed as

$$d\sigma = Kd\varepsilon_{v,t} \qquad (1)$$

where σ is the hydrostatic stress (the compressive direction is positive), K is bulk modulus, and $\varepsilon_{v,t}$ is the natural or true volumetric strain defined by [19]

$$d\varepsilon_{v,t} = -\frac{dV}{V} \qquad (2)$$

where V is the total volume of the material body under the current state of stress. In Eqs (1) and (2), a decrease in the volume is considered to be positive. Our hypothesis herein is that Hooke's law holds for natural strains in some regions of a rock body. In the literature of material science, Freed [19] provided a historical review of the development of the concept of natural strain and argued that the natural strain should be used for accurately describing material deformation.

In previous studies [16], the following definition of strain (so-called engineering strain $\varepsilon_{v,e}$) is often used when applying Hooke's law:

$$d\varepsilon_{v,e} = -\frac{dV}{V_0} \qquad (3)$$

where V_0 is the unstressed bulk volume. When the engineering strain is employed in Hooke's law, one can obtain the following relationship by integrating Eq (3) and using the condition that $V = V_0$ for $\sigma = 0$:

$$V = V_0(1 - \frac{\sigma}{K}) \qquad (4)$$

Similarly, the use of natural strain in Hooke's law [Eq. (2)] yields

$$V = V_0 \exp\left(-\frac{\sigma}{K}\right) \qquad (5)$$

It is easily seen that Eqs (4) and (5) are practically identical for small values of $\frac{\sigma}{K}$ (or strain).

In the literature of rock mechanicals, the engineering strain has been exclusively used considering that the elastic strain is generally small. Porous and fractured rock, however, differs from purely solid materials in that it is inherently heterogeneous and includes both solid phase and pores (and/or fractures) with a variety of geometric shapes. While the elastic strain is indeed small in most of the rock for stress changes of practical interest, the strain can be considerably large within some portions of a rock body. For example, some pores (or fractures) in a rock can be subject to significant deformation, and even completely closed under a certain range of stress changes encountered in practice. For these pores, the strain is not small (on the order of one). An accurate description of the deformation of this portion of the rock is important for coupled mechanical and hydrological processes, because fluid flow occurs in pores and fractures.

To deal with this issue, we conceptualize the heterogeneous rock as having two parts, and hypothesize that one part (a portion of pore volume or fracture apertures) obeys natural-strain-based Hooke's law, and the other part follows engineering-strain-based Hooke's law. For simplicity, the first part is called "soft" part and the other called "hard" part. This conceptualization can be represented by a hypothesized composite spring system shown in Fig 1. These two springs are subject to the same stress, but follow different varieties of Hooke's law. Berryman [20] also divided a poroelastic medium into "hard" and "soft" portions for the similar purpose in studying anisotropy of pore-fluid

enhanced shear modulus. In this study, we use subscripts 0, e, and t to denote the unstressed state, the hard part (where engineering-strain-based Hooke's law applies) and the soft part [where natural (or true)-strain-based Hooke's law applies], respectively, for a rock body. Then we have

$$V_0 = V_{0,e} + V_{0,t} \tag{6}$$

and

$$dV = dV_e + dV_t \tag{7}$$

Applying Eqs (4) and (5) to rock volumes V_e and V_t, respectively, in Eq (7) yields

$$-\frac{dV}{V_0} = \gamma_e \frac{d\sigma}{K_e} + \gamma_t \exp\left(-\frac{\sigma}{K_t}\right)\frac{d\sigma}{K_t} \tag{8}$$

$$\gamma_t = \frac{V_{0,t}}{V_0} \tag{9}$$

$$\gamma_e = 1 - \gamma_t \tag{10}$$

where K_e and K_t refer to bulk moduli for the hard and soft parts, respectively. Eqs (8)-(10) together comprise our proposed stress-strain relationship.

We should emphasize that our theory is a macroscopic-scale approximation that uses natural-strain-based Hooke's law to describe nonlinear deformation behavior of a fraction of pore volume (consisting of a collection of pores with a variety of geometry) subject to considerable deformation. This nonlinear deformation could result from combining effects of non-uniform pore size distributions and pore geometry heterogeneity [16]. A rough fracture can also be considered a collection of pores with different sizes and geometries for the purpose of deformation calculations. The validity of this approximation will be evaluated in the following sections.

3. Constitutive Relationships

In this section, we will use our newly developed stress-strain relationship to derive constitutive relationships between stress and mechanical/hydraulic properties for porous and fractured rock subject to elastic deformation. The derived relationships are also compared with the corresponding empirical expressions and experimental data.

3.1 Bulk rock compressibility

Bulk rock compressibility characterizes the capability for a rock body to deform when stress is changed under a constant pore-pressure condition. Mathematically, the bulk rock compressibility is defined by [16]:

$$C_{bc} = -\frac{1}{V_0}\frac{\partial V}{\partial \sigma} \tag{11}$$

Substituting Eq (8) into (11) yields

$$C_{bc} = \frac{\gamma_e}{K_e} + \frac{\gamma_t}{K_t}\exp\left(-\frac{\sigma}{K_t}\right) \tag{12}$$

The derived stress-compressibility relation consists of two terms. The first term is a constant; the second term is an exponential function. In fact, a number of researchers [12, 16, 21] have already noticed that rock compressibility data can often be empirically fitted to exponentially decreasing functions of the form:

$$C_{bc} = C_{bc}^{\ \infty} + (C_{bc}^{\ i} - C_{bc}^{\ \infty})\exp\left(-\frac{\sigma}{P}\right) \tag{13}$$

where the superscript i denotes the initial (zero stress) value, the superscript ∞ denotes the value at high stress, and P is considered as a characteristic stress. Based on certain assumptions, Jaeger et al. [16] rewrote the above equation as

$$C_{bc} = C_{bc}^{\infty} + \frac{\phi_{crack}}{P} \exp\left(-\frac{\sigma}{P}\right) \qquad (14)$$

where ϕ_{crack} refers to the porosity of crack-like voids in a porous rock sample. These voids were considered to be responsible for observed nonlinear deformation [16]. Zimmerman [12] fit measured compressibilities of three consolidated sandstones, Boise, Berea, and Bandera, to functions of the form of Eq (13). We refer the readers to Zimmerman [12] for details of the curve-fitted results.

Several interesting observations can be made when comparing our result [Eq (12)] with Eq (13) or (14). First, the functional forms of Eqs (12) and (14) are identical, indicating that our theoretical result is consistent with the corresponding empirical expressions and the related experimental data used to develop these expressions. Second, the curve-fitted results of Zimmerman [12] indicate that γ_t in Eq (12) [or ϕ_{crack} in Eq (14)] ranges from 0.2% to 0.5% for the three sandstones under consideration. It is much smaller than a typical porosity value for a sandstone rock (between 10% to 20%), suggesting that the so-called soft part of the rock body is only a small percentage of pore volume. This seems to be confirmed by the results to be discussed later in this study. Third, values for K_t for the three sandstones (4.74 to 8.33 MPa) are significantly smaller (by three orders of magnitude) than those for K_e (9.5 to 12.2 GPa), indicating that the part where natural strain should be used is significantly "softer" than the rest of the rock body. This is consistent with our theoretical argument that different varieties of Hooke's law should be used for different parts of porous and fractured rock. Note that the second term on the right hand side of Eq (12) is not necessarily smaller than the first one, especially for low stress states, although γ_t is generally small, as demonstrated in Fig 2.

3.2 Pore compressibility

The pore compressibility represents the change in pore volume per unit of stress change under a condition of constant pore pressure. Mathematically, this compressibility can be expressed by

$$C_{pc} = -\frac{1}{V_0{}^p}\frac{\partial V^p}{\partial \sigma} \tag{15}$$

where superscript p refers to pores. (The above equation holds for constant pore pressures.) Using similar notions from Section 2, we have

$$V_0{}^p = V_{0,e}{}^p + V_{0,t} \tag{16}$$

$$V^p = V_e{}^P + V_t \tag{17}$$

Note that in the above two equations, we consider V_t to be a portion of pore volume in a rock body. Following the same procedure to derive Eqs (3) and (4), we can obtain

$$dV_e{}^p = -C_e V_{0,e}{}^p d\sigma \tag{18}$$

$$dV_t = -\frac{V_{0,t}}{K_t}\exp\left(-\frac{\sigma}{K_t}\right)d\sigma \tag{19}$$

where C_e is the compressibility for the hard fraction of pore volume where engineering strain is applicable. This treatment is based on our argument that all the soft part corresponds to a fraction of pore volume.

Combining Eqs (15) to (19) yields

$$C_{pc} = C_{pc}{}^{\infty} + \frac{\gamma_t}{\phi_0 K_t}\exp\left(-\frac{\sigma}{K_t}\right) \tag{20}$$

where

$$C_{pc}^{\infty} = C_e \frac{V_{0,e}^{p}}{V_0^{p}} \tag{21}$$

$$\phi_0 = \frac{V_0^{p}}{V_0} \tag{22}$$

Eq (20) is used to fit one set of compressibility data (Fig 3) presented in Jaeger et al. [16]. This data set was derived from a measured relationship between pore strain and confining stress for a Frio sandstone from East Texas (after Carpenter and Spencer [22]). The match between Eq (20) and the data points is satisfactory, indicating that our derived result is able to capture key features of the experimental observations. The fitted parameter values are: C_{pc}^{∞} = 3.33 x 10^{-6} psi^{-1} = 4.83 x 10^{-4} MPa^{-1}, K_t = 1.1 x 10^3 psi = 7.6 MPa, and $\frac{\gamma_t}{\phi_0}$ =0.011. For typical porosity (ϕ_0) values of 10-20% for a sandstone, the γ_t value from pore compressibility data ranges from 0.11 to 0.22%, which again suggests that the so-called "soft" part is only a small percentage of pore volume. These parameter values are reasonably close to those obtained from rock compressibility data provided in the previous subsection.

3.3 Rock porosity

The rock porosity (ϕ) is a critical parameter for fluid flow in porous rock. Accurate descriptions of stress-dependent behavior for porosity are especially important for modeling coupled hydrological and mechanical processes. In this subsection, we derive a theoretical relationship between rock porosity and stress.

Using the same notations as in the previous subsection and by definition of rock porosity, we have

$$d\phi = \frac{dV^{p}}{V} = \frac{dV_e^{\,p} + dV_t}{V} \qquad (23)$$

where V is the bulk volume of porous rock. (Note that the above equation ignores the effect of V change with stress on porosity change.) For most practical applications of rock mechanicals, V can be approximated by the unstressed volume V_0 for calculating rock porosity. Using this approximation and Eqs (18) and (19), we obtain

$$d\phi = -\phi_e C_e d\sigma - \frac{\gamma_t}{K_t}\exp\left(-\frac{\sigma}{K_t}\right)d\sigma \qquad (24)$$

where

$$\phi_e = \phi_0 - \gamma_t \qquad (25)$$

Integrating Eq (24) and using $\phi = \phi_0$ for $\sigma = 0$ gives

$$\phi = \phi_e(1 - C_e\sigma) + \gamma_t \exp\left(\frac{\sigma}{K_t}\right) \qquad (26)$$

When the term of $C_e\sigma$ is much smaller than unity, the above equation can be approximately reduced to

$$\phi = \phi_e + \gamma_t \exp\left(-\frac{\sigma}{K_t}\right) \qquad (27)$$

Based on laboratory experiments on sandstone by Davis and Davis [23], Rutqvist et al. [7] proposed an empirical stress-porosity expression that is identical in form to Eq (27). Similar empirical expressions were originally reported by Athy [24] and further discussed in Neuzil [18]. In this study, the more general stress-porosity relation [Eq (26)]

is evaluated using data sets of Coyner [25]. He reported measured porosity-confining pressure (effective stress) relations for several types of rock. We select his laboratory measurements for Berea sandstone and Weber sandstone samples, because these rock samples exhibit a relatively large degree of stress dependence. Note that confining pressure is used here to approximate the effective stress, since Biot coefficients are close to one for the two sandstones under consideration [17].

There are four parameters in Eq (26): ϕ_e , C_e, γ_t and K_t. To avoid the non-uniqueness of parameter values determined from curve fitting, we use a simple procedure to estimate parameter values from porosity vs. confining pressure data. As shown in Figs 4 and 5, measured relations between porosity and confining pressure are very well represented by a straight line for relatively high pressures (stresses). The slope of the straight line is used to determine $\phi_e C_e$ because the second term on the right hand side of Eq (26) is negligible for high stress values. The porosity value at the intersection between the straight line and the vertical axis in Fig 4 or 5 gives ϕ_e value, considering that the straight line represents the first term on the right hand side of Eq (26). The measured porosity value at zero pressure is equal to $\phi_e + \gamma_t$, as implied from Eq (26). The above procedure allows for direct determination of values for ϕ_e , C_e and γ_t. The remaining parameter K_t can be estimated using porosity data at relatively low pressures. In this study, a K_t value is simply calculated from Eq (26) using measured porosity value at a pressure of 10 MPa.

Satisfactory matches between results calculated from Eq (26) (with determined parameter values) and porosity data are shown in Figs 4 and 5. The estimated parameter values for Berea sandstone are ϕ_e = 17.52%, $C_e = 3.04 \times 10^{-4}$ (MPa^{-1}), γ_t = 0.28% and K_t

= 9.97 MPa. The parameter values for Weber sandstone are ϕ_e = 9.00 %, C_e = 2.96 x 10^{-4} (MPa^{-1}), γ_t = 0.48 % and K_t = 10.60 MPa. Note that the values for γ_t and K_t are generally consistent with those reported in the previous sections where the values for these parameters are estimated from different types of data. This indicates that these two parameters (introduced in this study) are very well defined and experimentally robust.

To further validate our theory, we use parameter values estimated from porosity data to calculate relations between the bulk-modulus and pressure (stress) and check if the calculated results can match the measured bulk modulus data for the same rock samples used for measuring porosity values [25]. From our stress-strain relationship [Eq (8)], the bulk modulus K can be given by

$$K = \frac{1}{\frac{\gamma_e}{K_e} + \frac{\gamma_t}{K_t}\exp\left(-\frac{\sigma}{K_t}\right)} \qquad (28)$$

The above equation can also be derived from Eq (12). Values for $\frac{K_e}{\gamma_e}$ correspond to K values for high stresses (pressures) and must be determined from measured K data. (They cannot be determined from porosity data.) Based on data shown in Figs 6 and 7, the value of $\frac{K_e}{\gamma_e}$ is set to 13.5 GPa for Berea sandstone and 17.5 GPa for Weber sandstone. As shown in Figs 6 and 7, the calculated results are in a good agreement with data. This is encouraging (considering that a curve-fitting procedure is not used in these two figures) and also supports the robustness of our theory.

3.4 Fracture aperture

Fracture aperture is an important parameter for both mechanical and hydraulic processes within a fractured rock. For example, fracture permeability is largely determined by fracture aperture. A number of empirical expressions exist in the literature for describing observed relations between normal stress and fracture closure (that is linearly related to the average fracture aperture) [26,27]. In this subsection, we develop a relationship for the dependence of fracture aperture on the normal stress based on the proposed stress-strain relationship.

Consider a fracture to be embedded into a rock sample subject to a normal stress σ_n. We again divide fracture space into "hard" and "soft" parts along the direction normal to the fracture plane. Then, the volumetrically averaged fracture aperture (b) is given by

$$b_0 = b_{0,e} + b_{0,t} \tag{29}$$

under unstressed conditions, and

$$b = b_e + b_t \tag{30}$$

under stressed conditions. Similar to previous sections, superscripts e and t refer to the "hard" and "soft" parts in a fracture. Hooke's law for the two parts can be expressed by

$$d\sigma_n = -K_{F,e}\frac{db_e}{b_{0,e}} \tag{31}$$

$$d\sigma_n = -K_{F,t}\frac{db_t}{b_t} \tag{32}$$

where subscript F refers to fracture. (For convenience, the volumetric strain will not be used here.) Note that the stress in the above two equations refers to far-field normal stress, rather than local stress.

Combining Eqs (30) to (32) gives

$$db = db_e + db_t = -b_{0,e}\frac{d\sigma_n}{K_{F,e}} - b_t\frac{d\sigma_n}{K_{F,t}} \tag{33}$$

Integrating the above equation and using Eq (29) and the following relationship obtained from Eq (32):

$$b_t = b_{0,t}\exp\left(-\frac{\sigma_n}{K_{F,t}}\right) \tag{34}$$

one can obtain

$$b = b_{0,e}(1-\frac{\sigma_n}{K_{F,e}}) + b_{0,t}\exp\left(-\frac{\sigma_n}{K_{F,t}}\right) \tag{35}$$

In the above equation, the stress-dependent behavior of fracture aperture is controlled by the second term at low stress and the first term at high stress. Because $K_{F,e}$ is much larger than $K_{F,t}$, aperture change with stress will be much more gradual at high stress. This result is consistent with the observations of Pyrak-Nolte et al. [28], that the increase of fracture closure (or decreasing of fracture aperture) with increasing normal stress becomes more gradual, but does not reach zero, and even at considerably high stresses, a number of voids remain open. Nevertheless, there is a considerable amount of laboratory data indicating that fracture closure (or fracture aperture) remains practically unchanged at high stress [26,27]. This is equivalent to saying that the following condition holds in practice:

$$1-\frac{\sigma_n}{K_{F,e}} \approx 1 \tag{36}$$

In this case, we can reduce Eq (35) to

$$b = b_{0,e} + b_{0,t} \exp\left(- \frac{\sigma_n}{K_{F,t}} \right) \qquad (37)$$

This equation is identical to the empirical expression of Rutqvist et al. [7] for the stress-fracture aperture relationship. The expression has been used successfully to match laboratory measurements. For example, Fig 8 shows the match of Eq (37) to the measurements of the third loading-unloading cycle for a fracture [29]. Some hysteresis exists. Barton et al. [27] suggested that the hysteresis was a laboratory artifact and that *in situ* fractures probably also behave in a manner similar to that observed from the third or fourth loading cycles.

The consistency of our Eq (36) with the empirical expression of Rutqvist et al. [7] is encouraging. Fig 8 shows that unlike the "soft" part of porous rock, the "soft" part in a fracture corresponds to a relatively large portion of fracture voids. This may result from a geometric difference between fractures and rock pores. Previous studies [30] demonstrate that a rock "crack" with a smaller aspect ratio (ratio of thickness to length) is more easily deformed than that with a smaller ratio. Obviously, values for the ratio are much larger for fractures than those for most pores in a porous rock. Fig 8 also shows the modulus for the fracture ($K_{F,t}$) is in the range of 2-4 MPa, and smaller than the previously reported modulus values for the soft part of the porous rock. This is consistent with an intuitive expectation that a fracture is "softer" than pores in porous rock.

4. Concluding Remarks

This study develops a general stress-strain relationship for porous and fractured rock subject to elastic mechanical deformation, based on the hypothesis that different varieties of Hooke's law need to be employed for different parts of a rock body, for describing the

elastic mechanical deformation. The stress-strain relationship developed here allows for the derivation of constitutive relationships between stress and a number of mechanical/hydraulic properties. The remarkable consistency between these relationships and a variety of the corresponding empirical expressions and/or laboratory experimental data supports the validity of our theoretical development. The parameter values estimated from different kinds of measurements are also close for similar rocks, indicating that newly introduced parameters are well defined and robust for the applications considered.

The focus of this paper has been on the presentation of a theoretical framework. Our preliminary evaluation produced encouraging results. Further work is still needed to validate our theory using more comprehensive comparisons between our results and those of different types of mechanical data. Also, it is both desirable and of practical interest to explore possible correlations among parameters characterizing the soft part of a rock, rock type, and the other associated rock properties. Important examples of related properties are electrical resistivity/conductivity data for fluid-saturated porous rocks [31,32,33] and also permeability data [34].

Acknowledgement

We are indebted to Seiji Nakagawa at Lawrence Berkeley National Laboratory for his critical and careful review of a preliminary version of this manuscript. This work was supported by the U.S. Department of Energy (DOE), under DOE Contract No. DE-AC02-05CH11231.

References

[1] Rutqvist J, Stephansson O. The role of hydromechanical coupling in fractured rock engineering. Hydrogeology J 2003; 11: 7-40.

[2] Pine RJ, Batchelor AS. Downward migration of shearing in joined rock during hydraulical injections. Int J Rock Mech Mining Sci 1984; 21:249-263.

[3] Baria R, Baumgartner J, Rummel F, Pine RJ, Sato Y. HDR/HWR reservoirs: concepts, understanding and creation. Geothermics 1999;28:533-552.

[4] Lewis RW, Schrefler BA. The finite element method in the static and dynamic deformation and consolidation of porous media, 2nd edn. Wiley, New York. 1998.

[5] Tsang C-F. Introduction to coupled processes. In: Tsang C-F (ed) Coupled processes associated with nuclear waste repositories. Academic Press, Orlando. 1987.

[6] Rutqvist J, Tsang C-F. Analysis of thermal-hydrologic-mechanical behavior near an emplacement drift at Yucca Mountain. J. Contaminant Hydrol 2003; 62-3: 637-652.

[7] Rutqvist J, Wu Y-S, Tsang C-F, Bodvarsson G. A modeling approach for analysis of coupled multiphase fluid flow, heat transfer, and deformation in fractured porous rock. Int J Rock Mech Mining Sci 2002; 39:429-442.

[8] Apps J, Tsang C-F. Preface. In: Apps J, Tsang C-F (eds) Deep injection of disposal of hazardous industrial waste. Scientific and engineering aspects. Academic Press, San Diego, California. 1996.

[9] Brasier FM, Kobelsky BJ. Injection of industrial wastes in the United States. In: Apps J, Tsang C-F (eds) Deep injection of disposal of hazardous industrial waste. Scientific and engineering aspects. Academic Press, San Diego, California. 1996.

[10] Jing L, Hudson JA. Numerical methods in rock mechanicals. Int J Rock Mech Mining Sci 2002; 39:409-427.

[11] Mavko G, Nur A. Melt squirt in the asthenosphere. J.Geophys. Res. 1978;80:1444-1448.

[12] Zimmerman RW. Compressibility of Sandstones. Elsevier, Amsterdam. 1991.

[13] Walsh JB. The effect of cracks on the compressibility of rock. J.Geophys. Res. 1965;70:381-389.

[14] Walsh JB. The effect of cracks on the uniaxial elastic compression of rocks. J.Geophys. Res. 1965;70:399-411.

[15] Nur A. Effects of stress on velocity anisotropy in rocks with cracks. J.Geophys. Res. 1971;76:2022-2034.

[16] Jaeger JC, Cook NGW, Zimmerman RW. Fundamentals of rock mechanicals (4th Edn). Backwell Publishing. 2007.

[17] Berryman JG. Effective stress for transport properties of inhomogeneous porous rock. Journal of Geophysical Research 1992; 97 (B12): 17409-17424.

[18] Neuzil CE. Hydromechanical coupling in geologic processes. Hydrogeology Journal. 2003; 11: 41-83.

[19] Freed AD. Natural Strain. J. Eng. Mater. Technol. 1995;117:379-385.

[20] Berryman JG. Estimates and rigorous bounds on pore-fluid enhanced shear modulus in poroelastic media with hard and soft anisotropy. 2006; 15: 133-167.

[21] Wyble DO. Effect of applied pressure on the conductivity, porosity, and permeability of sandstones. Petrol Trans AIME 1958; 213: 430-432.

[22] Carpenter CB, Spencer GB. Measurement of compressibility of consolidated oil-bearing sandstones. Report 3540. U.S. Bureau of Mines, Denver. 1940.

[23] Davis JP, Davis DK. Stress-dependent permeability: characterization and modeling. Society of Petroleum Engineers, SPE paper no. 56813, 1999.

[24] Athy LF. Density, porosity, and compaction of sedimentary rock. Am. Assoc. Pet. Geol. Bull. 1930; 14: 1-24.

[25] Coyner KB. Effects of stress, pore pressure, and pore fluids on bulk strain, velocity, and permeability of rocks. Ph.D. thesis. Mass. Inst. Of Technol., Cambridge, 1984.

[26] Goodman RE. Methods of geological engineering in discontinuous rocks. West Publishing, New York. 1976.

[27] Barton NR, Bandis SC, Bakhtar K. Strength, deformation, and conductivity coupling of rock joint deformation. Int J Rock Mech 1985; 22: 121-140.

[28] Pyrak-Nolte LJ, Myer LR, Cook NGW, Witherspoon PA. Hydraulical and mechanical properties of natural fractures in low permeability. In: Herget G, Vongpaisal S., editors. Proceedings of the Sixth International Congress on Rock Mechanicals. Canada, Balema, 1987.

[29] Liu HH, Rutqvist J, Zhou Q, Bodvarsson GS. Upscaling of Normal stress-permeability relationships for fracture networks obeying the fractional Levy motion. In:

Stephansson O, Hudson JA, Jing L. editors. Coupled Thermo-Hydro-Mechanical-Chemical Processes in Geo-Systems: Fundamentals, Modeling, Experiments and Applications. Elservier. 2004.

[30] Kachanov M. Elastic solids with many cracks and related problems. Adv Appl Mech 1994; 30: 259-445.

[31] Brace, W. F., Orange, A. S., and Madden, T. R., The effect of pressure on the electrical resistivity of water-saturated crystalline rocks, J. Geophys. Res. 1965; 70, 5669—5678.

[32] Brace, W. F., and Orange, A. S., Electrical resistivity in saturated rock under stress, Science 1966; 153, 1525—1526.

[33] Brace, W. F., and Orange, A. S., Further studies of the effects of pressure on electrical resistivity of rocks, J. Geophys. Res. 1968; 73, 5407—5419.

[34] Brace, W. F., Walsh, J. B., and Frangos, W. T., Permeability of granite under high pressure, J. Geophys. Res. 1968; 73, 2225—2236.

Figures

Fig. 1. A composite spring system consisting of two springs. The hard and soft springs follow engineering-strain-based and natural-strain-based Hooke's law, respectively.

Fig. 2. Bulk compressibility as a function of stress calculated from Eq (14) using the fitted parameter values (C_{bc}^{∞} = 0.082 GPa^{-1}, P=8.33 MPa and ϕ_{crack} =0.0044) reported by Zimmerman [12].

Fig. 3. Match of Eq (20) to the data points of pore compressibility (10^{-6}/psi) as a function of confining pressure (or stress) (psi) presented in Jaeger et al. [16].

Fig. 4. Match between porosity values (as a function of confining pressure) calculated from Eq (26) and the measured data for Berea Sandstone [25].

Fig. 5. Match between porosity values (as a function of confining pressure) calculated from Eq (26) and the measured data for Weber Sandstone [25].

Fig. 6. A comparison between bulk modulus values (as a function of confining pressure) calculated from Eq (26) and the measured data for Berea Sandstone [25].

Fig. 7. A comparison between bulk modulus values (as a function of confining pressure) calculated from Eq (26) and the measured data for Weber Sandstone [25].

Fig. 8. Matches of Eq (36) to the observed stress-aperture data points for a fracture. The fitted parameter values are $b_{0,e}$=3 μm, $b_{0,t}$=23 μm, and $K_{F,t}$ = 3.3 MPa and 2.2 MPa, respectively, for the loading and unloading data points.

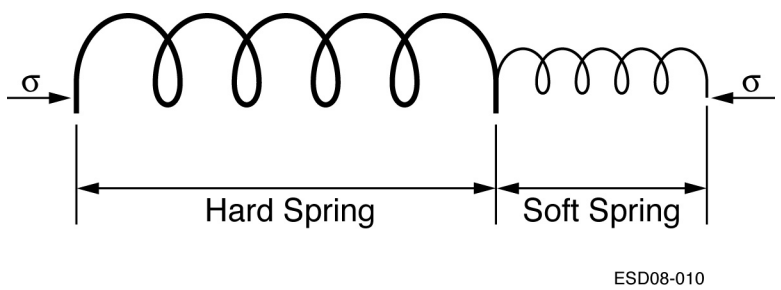

Fig. 1. A composite spring system consisting of two springs. The hard and soft springs follow engineering-strain-based and natural-strain-based Hooke's law, respectively.

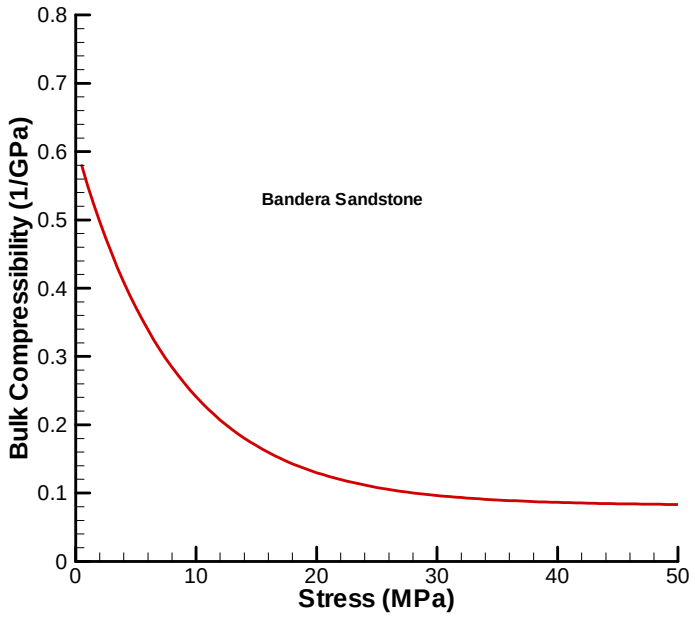

Fig. 2. Bulk compressibility as a function of stress calculated from Eq (14) using the fitted parameter values (C_{bc}^{∞} = 0.082 GPa^{-1}, P=8.33 MPa and ϕ_{crack} =0.0044) reported by Zimmerman [12]

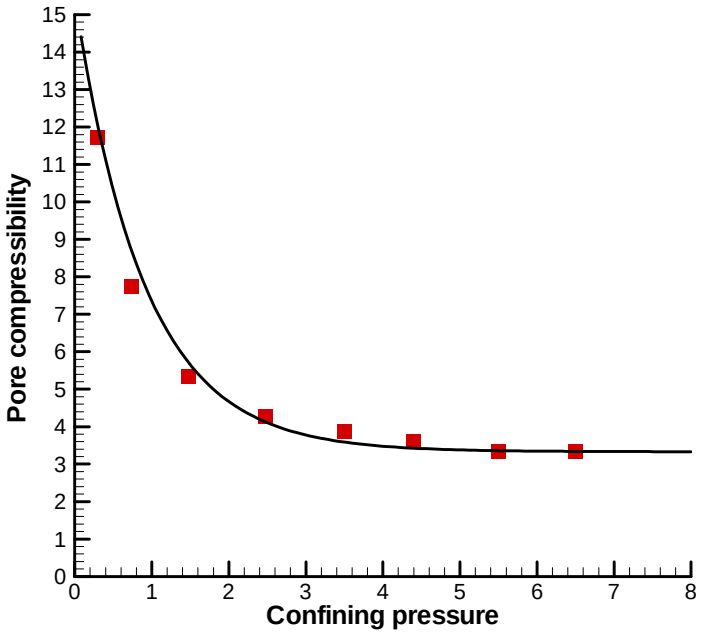

Fig. 3. Match of Eq (20) to the data points of pore compressibility (10^{-6}/psi) as a function of confining pressure (or stress) (psi) presented in Jaeger et al. [16].

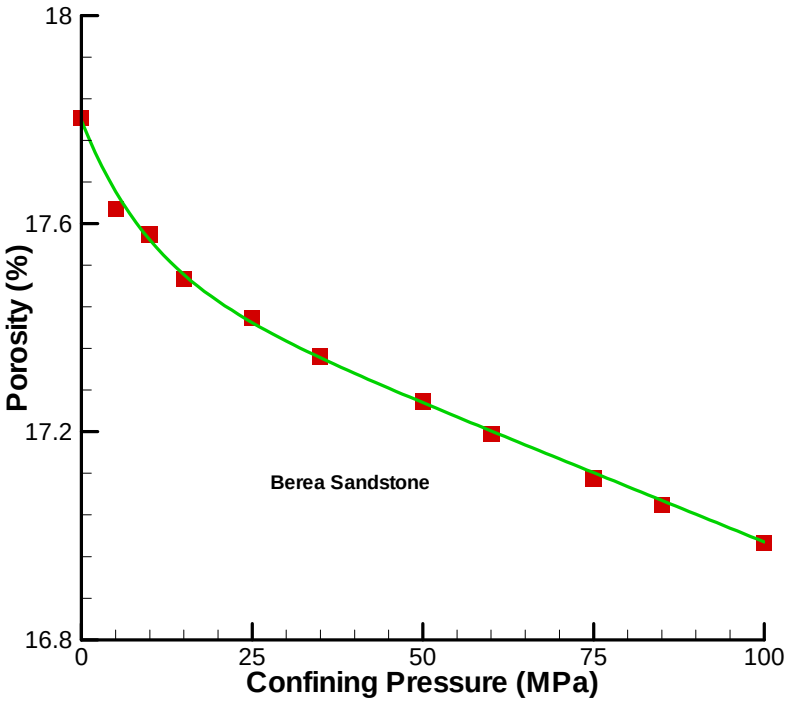

Fig. 4. Match between porosity values (as a function of confining pressure) calculated from Eq (26) and the measured data for Berea Sandstone [25].

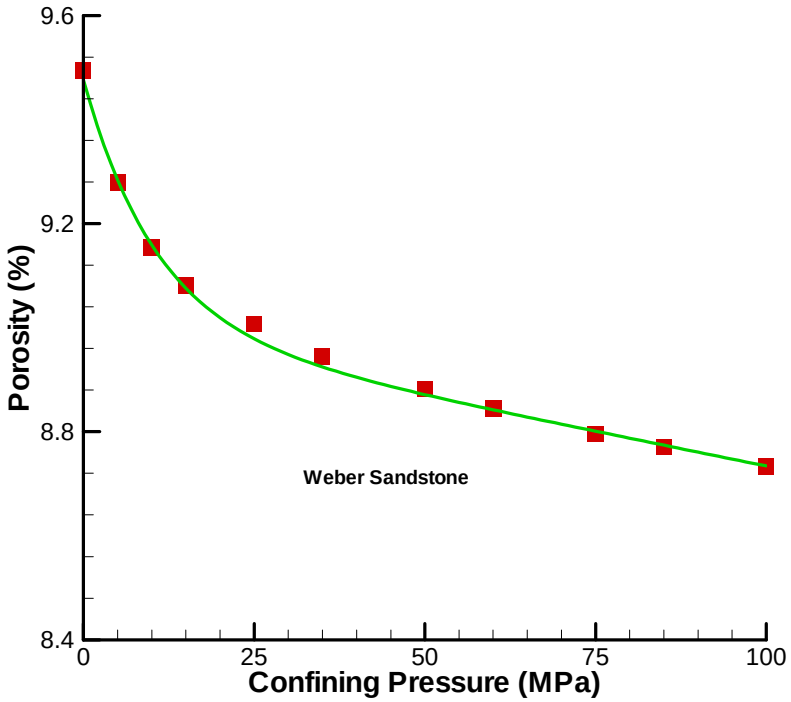

Fig. 5. Match between porosity values (as a function of confining pressure) calculated from Eq (26) and the measured data for Weber Sandstone [25].

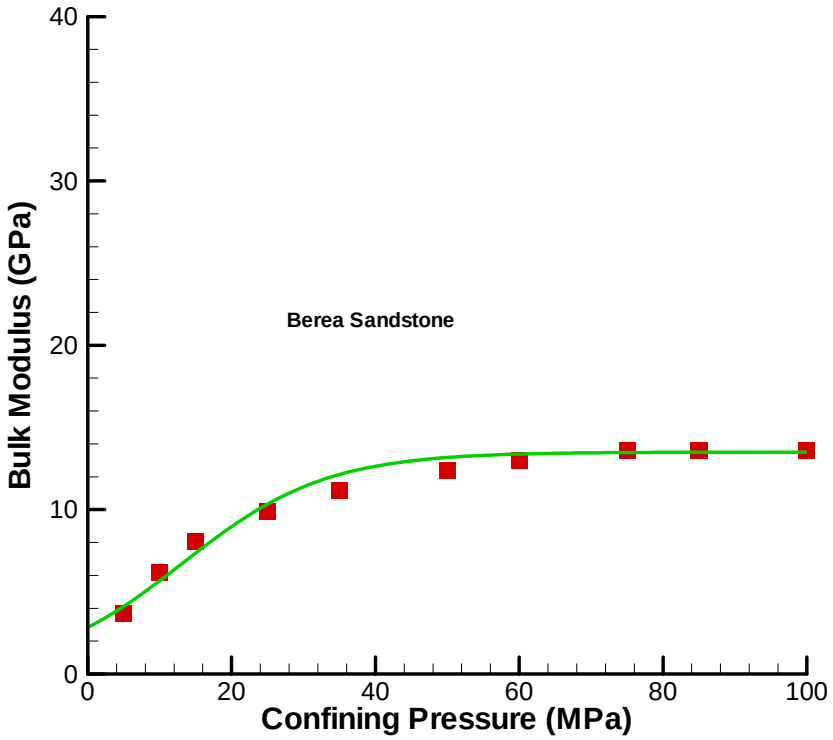

Fig. 6. A comparison between bulk modulus values (as a function of confining pressure) calculated from Eq (26) and the measured data for Berea Sandstone [25].

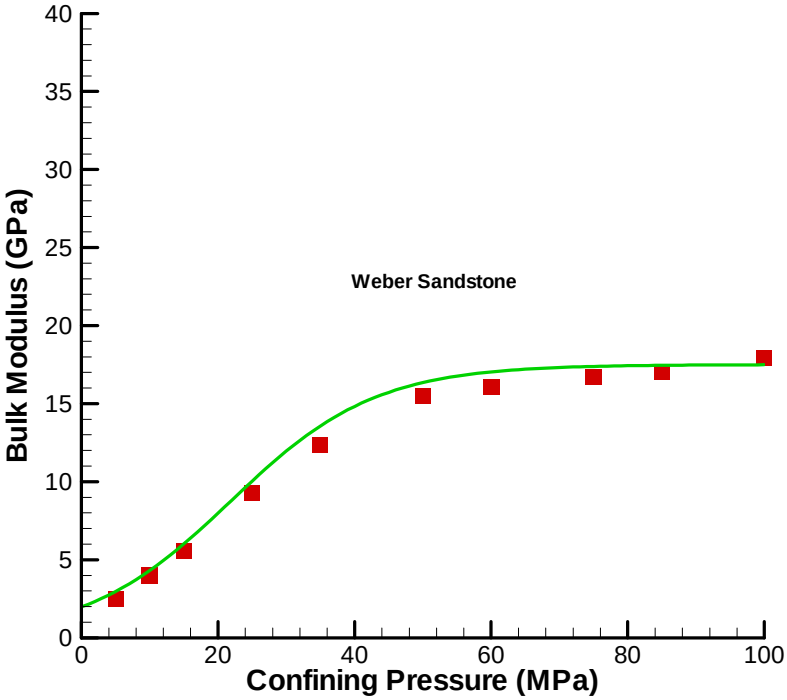

Fig. 7. A comparison between bulk modulus values (as a function of confining pressure) calculated from Eq (26) and the measured data for Weber Sandstone [25].

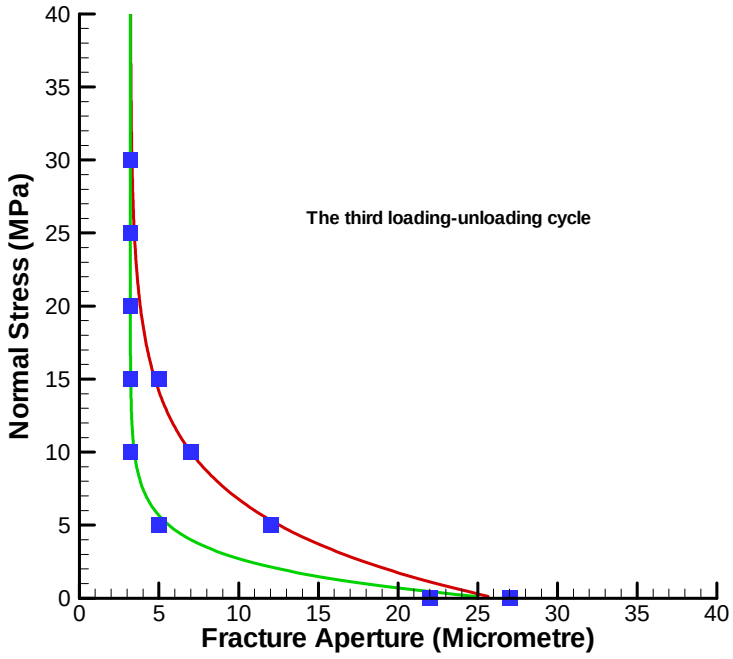

Fig. 8. Matches of Eq (36) to the observed stress-aperture data points for a fracture. The fitted parameter values are $b_{0,e}$=3 μm, $b_{0,t}$=23 μm, and $K_{F,t}$ = 3.3 MPa and 2.2 MPa, respectively, for the loading and unloading data points.